Catalysis Letters (2022) 152:75–86
https://doi.org/10.1007/s10562-021-03626-4

Kinetics Study of the Esterification Reaction of Cyclohexene to Cyclohexyl Acetate Catalyzed by Novel Brønsted–Lewis Acids Bifunctionalized Heteropolyacid Based Ionic Liquids Hybrid Solid Acid Catalysts

Binxiong Guang[1] · Yuefeng Wu[1] · Weihua Liu[1] · Jianhong Wang[1] · Yahui Xiao[1] · Yong Liu[1]

Received: 8 February 2021 / Accepted: 9 April 2021 / Published online: 20 April 2021

Abstract

A series of Brønsted–Lewis acids bifunctionalized heteropolyacid based ionic liquids hybrid solid acid catalysts (BLA-HPA-ILs) were synthesized by combining the Brønsted acidic ionic liquid [Bis–Bs–BDMAEE]$HPW_{12}O_{40}$ with metallic oxide in different composition ratios and applied in the esterification of cyclohexene to cyclohexyl acetate. Among the synthesized catalysts, the $^{1}/_{2}$Cu[Bis–Bs–BDMAEE]$HPW_{12}O_{40}$ catalyst with Brønsted and Lewis acidities shown the most excellent catalytic performance for the esterification of cyclohexene with acetic acid. The BLA-HPA-ILs catalysts were characterized by elemental analysis, FT-IR, Py-IR, TG, ^{1}H NMR, SEM and EDX. The effects of reaction temperature, catalyst dosage, and initial reactant molar ratio has been investigated in detail. A pseudohomogeneous (PH) kinetic model was used to correlate the kinetic data in the temperature range of 333.15–363.15 K, and the kinetic parameters were estimated, indicating the results calculated by the kinetic model are well coincidence with the experimental results. Moreover, as a heterogeneous reaction catalyst, $^{1}/_{2}$Cu[Bis–Bs–BDMAEE]$HPW_{12}O_{40}$ could be easily recovered by a simple treatment and reused six times without any obvious decrease in catalytic activity, displaying good reusability.

Graphic Abstract

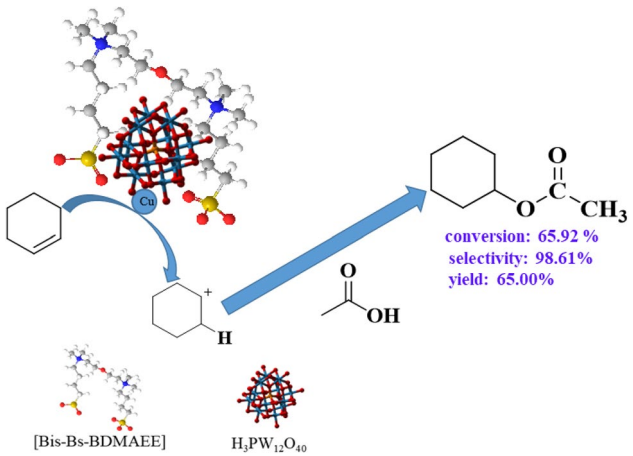

Keywords Heterogeneous catalysis · Ionic liquids · Bifunctionality · Kinetic modeling · Cyclohexene esterification

✉ Jianhong Wang
jhwnj@163.com

✉ Yong Liu
liuyong79@126.com

Extended author information available on the last page of the article

Abbreviations

A	Cyclohexene
B	Acetic acid
D	Cyclohexyl acetate

HPA	Heteropolyacid
ILs	Ionic liquids
HPA-ILs	Heteropolyacid based ionic liquids hybrid
BLA-ILs	Brønsted–Lewis acidic ILs
BLA-HPA-ILs	Brønsted–Lewis acids bifunctionalized heteropolyacid based ionic liquids hybrid solid acid
[Bis–Bs–BDMAEE]	$[HO_3S–(CH_2)_4–BDMAEE–(CH_2)_4–SO_3H]$
PH	Pseudohomogeneous
K_e	Equilibrium constant
k_+	Forward reaction rate constant (mol^{-1} min^{-1})
k_-	Reverse reaction rate constant (mol^{-1} min^{-1})
k_0	Pre-exponential factor (L^2 mol^{-2} min^{-1})
C_i	The molar concentration of component i (mol L^{-1})
m_{cat}	The catalyst dosage per unit volume (g L^{-1})
T	Temperature (K)
t	Time (min)
$\Delta_r H_0$	The reaction enthalpy (kJ mol^{-1})
$\Delta_r S$	Entropy (J mol^{-1} K^{-1})
x	Conversion of cyclohexene
x_{cal}	Calculated conversion
x_{exp}	Experimental conversion
E_a	Activation energy (kJ mol^{-1})
SRS	Minimum sum of residual squares

1 Introduction

Cyclohexanol is the intermediate raw material in the production of caprolactam, adipate and other phthalamide products, which has been widely used in organic chemicals, coating, and textile industries [1]. There are three main methods to produce cyclohexanol including the oxidation of cyclohexane, the hydrogenation of phenol, and the direct hydration of cyclohexene [2–5]. Up to now, the oxidation of cyclohexane to produce cyclohexanol is a main method in industry. However, this method suffers from several drawbacks which limit its development [6], including limited selectivity, high energy consumption, and explosion hazards. In addition, the hydrogenation of phenol develops slowly due to the high cost of phenol and the large demand of hydrogen energy [7]. In the above method, the direct hydration of cyclohexene to produce cyclohexanol is a promising method owing to its advantages of atom economy, and high selectivity [8]. Unfortunately, the direct hydration reaction is still limited by low reaction rate because of the extremely poor miscibility between cyclohexene and water, which is only 0.02% (w/w) at 298 K [9]. Hence, the establishment of a new technology to replace direct hydration has become especially important.

A two-step indirect hydration method for cyclohexanol has been developed to overcome the above shortcomings of direct hydration method for cyclohexene [10]. For the first step, the cyclohexyl carboxylate is formed by the reaction of cyclohexene with the carboxylic acid (e.g. formic acid, acetic acid, etc.), which is an electrophilic addition esterification using acid catalyst [11]. In the second step, the ester can be produced cyclohexanol by hydrolysis, transesterification, or hydrogenation [12]. Steyer and co-workers [13] have confirmed the feasibility of this route by the esterification of cyclohexene with formic acid and the subsequent hydrolysis of the ester in a reactive distillation column. The catalytic reaction distillation process has been used in the indirect hydration process for the production of cyclohexanol [14, 15]. It is particularly worth mentioning that the esterification of cyclohexene with carboxylic acid to form cyclohexyl carboxylate is the decisive step in the entire indirect hydration process [16]. In other words, the yield of the target product cyclohexanol can be increased by increasing the esterification reaction rate of cyclohexene. Until now, various catalysts such as strong cation exchange resins Amberlyst-15 have been applied in the esterification of cyclohexene [11, 17]. However, the conversion rate of cyclohexene is relatively low with the conventional solid acid catalyst in the esterification of cyclohexene and formic acid [18–20]. Thus, it is particularly important to increase the activity of the catalysts used in the esterification.

In recent years, functionalized ionic liquids (ILs), as a new type of clean catalyst and an excellent solvent, have attracted extensive research interest of scholars from various fields due to their distinguishing properties such as negligible vapor pressure, remarkable solubility, designability of molecules and high chemical stability [21–24]. ILs have been extensively applied in the esterification, hydrolysis, transesterification, and gas adsorption reaction because of their excellent catalytic activities [25–29]. However, the ILs have several drawbacks such as a large amount of ILs needed in reaction, and the difficult recovery of ILs from the reactants, which hinder their practical applications [30]. On the other hand, heteropolyacid (HPA) with Keggin structures have been widely applied in the many organic reactions due to their excellent catalytic performances. Whereas, there are many defects including the low surface area and solubility, which have limited its practical application [31, 32]. In order to overcome these drawbacks, immobilization of HPA could be an effective way to improve their catalytic performance [33]. Nonetheless, immobilization of HPA onto the different supports suffers from the slow reaction rate, and leaching of active sites [34, 35]. As a novel type of ionic liquids, heteropolyacid based ionic liquids hybrid (HPA-ILs) were

proposed by combining the ionic liquids with the heteropolyacid hybrid, which have received widespread attention because they not only have excellent catalytic performance, but also easy reuse in a solid state [36, 37]. HPA-ILs have been applied for esterification, hydroxylation, desulfurization, and oxidation reactions as catalysts [38–41]. In our previous works, many HPA-ILs catalysts have been synthesized and used in the esterification [42], transesterification [43] and hydrolysis [44].

Acidic ILs can be classified into Brønsted [45, 46] and Lewis types [47] in accordance with their acidic groups. As the novel catalysts, Brønsted–Lewis acidic ILs (BLA-ILs) which combined the exceptional performance of Lewis and Brønsted acid sites, have been developed and applied in many chemical reactions. Han et al. [48] assessed the catalytic activity of various [HO_3S-pmim]Cl-x$SnCl_2$(x = 0–0.8 mol) by transesterification reaction of soybean oil with methanol, a satisfactory biodiesel yield of 98.6% was achieved under optimized reaction conditions. The alkylation of isobutene or isobutene was investigated [49] in the presence of Brønsted–Lewis acidic ILs [$HO_3SC_3NEt_3$]Cl-$ZnCl_2$, exhibiting an outstanding catalytic performance. Yuan et al. [50] reported a heteropolyacid hybrid organic–inorganic catalyst $Sm_{0.33}[TEAPS]_2PW_{12}O_{40}$ by adding Sm^{3+} as the Lewis acid sites on the basis of functionalized Brønsted heteropolyacid hybrid ionic liquids $[TEAPS]_3PW_{12}O_{40}$, was used to catalyze the dimerization of rosin. This is because the Brønsted and Lewis acid sites and their covalent or ionic bonding modes are effective for the synergistic catalysis of the catalyst body in the solid–liquid system. Moreover, in our previous work, a series of Brønsted–Lewis acids bifunctionalized ionic liquids based heteropolyacid hybrid was prepared and shown excellent in the esterification reaction of camphene with acetic acid to produce isobornyl acetate [51].

Based on our study on the ILs and HPA catalysts, a series of BLA-HPA-ILs was prepared through anion exchange and the introduction of different metals (Cu, Co, Ni, etc.). These catalysts contained the advantages of ILs, HPAs and Brønsted–Lewis acid sites, and applied in esterification reaction of cyclohexene and acetic acid. The impact of various parameters of catalyst type, reaction temperature, initial reactant molar ratio and catalyst dosage was investigated in detail. A pseudohomogeneous (PH) kinetic model was applied to correlate the experimental data, and the corresponding kinetic parameters were estimated simultaneously.

2 Experimental

2.1 Materials

Phosphotungstic acid ($H_3PW_{12}O_{40}$), phosphomolybdic acid ($H_3PMo_{12}O_{40}$), silicotungstic acid ($H_4SiW_{12}O_{40}$), cyclohexene (≥ 99%) and acetic acid (≥ 99.5%) were supplied by Sinopharm Chemical Reagent, Shanghai, China. Bis(2-dimethylaminoethyl) ether (≥ 98%) was purchased from J&K Scientific Ltd., Beijing, China. 1,4-Butyl sultone (≥ 99%) was purchased by Aladdin Reagent Co., Ltd., Shanghai, China. All the chemicals were analytical pure and were directly used without further treatment.

2.2 Preparation of BLA-HPA-ILs

In this work, the novel BLA-HPA-ILs were synthesized by combining the sulfonic acid-functionalized ionic liquids based heteropolyacid hybrid [Bis–Bs–BDMAEE]$HPW_{12}O_{40}$ with CuO (Scheme 1).

The detailed synthesis procedure of [Bis–Bs–BDMAEE]$HPW_{12}O_{40}$ were according to our previous work [41]: Bis(2-dimethylaminoethyl) ether (0.1 mol) and 1,4-butyl sultone (0.21 mol) was added into a 100 mL flask. Then, the mixtures were placed in a water bath to 60 °C,

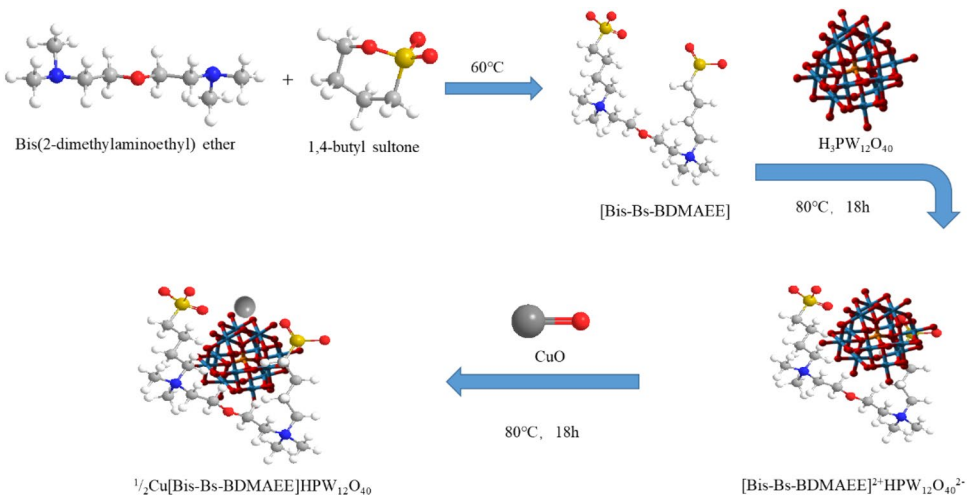

Scheme 1 The preparation process of $^1/_2$Cu[Bis–Bs–BDMAEE]$HPW_{12}O_{40}$

and agitated for 1 h. Afterwards, a white solid zwitterion [Bis–Bs–BDMAEE] was formed, and the unreacted components were removed by repeated washing with ether for 3 times, then dried in a vacuum at a reduced pressure of 80 °C. Next, a certain amount of an aqueous solution of $H_3PW_{12}O_{40}$ was added drop by drop. After that, the mixtures were placed in 80 °C water bath, refluxed and agitated for 18 h. After the reaction, the samples were filtered, washed, and dried under a vacuum to obtain the product [Bis–Bs–BDMAEE] $HPW_{12}O_{40}$. And then, [Bis–Bs–BDMAEE]$HPW_{12}O_{40}$ was dissolved in aqueous solution and added varied amounts of CuO. The mixtures were constant agitation till the solid was completely dissolved. The final $^1/_2$Cu[Bis–Bs–BDMAEE] $HPW_{12}O_{40}$ catalysts were obtained by using the rotary evaporator to remove water. [Bis–Bs–BDMAEE]$HPMo_{12}O_{40}$, [Bis–Bs–BDMAEE]$H_2SiW_{12}O_{40}$, and BLA-ILs-HPA doping other metallic oxide (M = Co, Ni, Zn, Fe, Al) were also prepared by the above description.

2.3 Characterization Methods

Fourier transform infrared spectroscopy (FT-IR) was measured using Vertex 70 (Bruker Optics, Germany), using KBR compression method, and the scanning range was 4000–450 cm^{-1}. The thermogravimetric analysis (TG) was measured within the range of 20–1000 °C using DSC851E (Mettler Toledo, Switzerland). The test conditions were high purity nitrogen atmosphere and the heating rate was 10 °C min^{-1}. Scanning electron microscope (SEM) and X-ray energy spectrum (EDX) were measured by JSM-7610F (JEOL, Japan). Elemental analysis (C, S, H, O, N) of the BLA-HPA-ILs catalysts were conducted with an elemental analyzer (Vario EL cube, Elemental Analysis System GmbH, Hanau, Germany). Nuclear magnetic resonance profile (NMR) was determined using an Avance 400 NMR instrument (Bruker AXS, Germany). ^{1}H NMR (Bruker DPX-400) characterization results for these catalysts were similar. Here only the representative data of [Bis–Bs–BDMAEE]$HPW_{12}O_{40}$ was given. ^{1}H NMR (400 MHz, D_2O) δ 1.70–1.82 (m, 4H), 1.88–2.04 (m, 4H), 2.91 (t, J = 7.6 Hz, 4H), 3.20 (s, 12H), 3.40 (t, J = 5.4 Hz, 4H), 3.69 (s, 4H), 4.09 (s, 4H).

2.4 Apparatus and Procedure

A round-bottom flask (50 mL) was placed in a constant temperature water bath of 363.15 K. 0.03 mol cyclohexene and 0.09 mol acetate acid were added to the flask. After the reactants reached the reaction temperature. The agitator and time measurement were started immediately when 0.55 g of BLA-ILs-HPA catalysts were added to the flask. The reaction was carried out for 9 h with stirring, samples were taken out from the reactor in specific intervals, and then rapidly put it to an ice bath to avoid its further reaction in each experiment. These samples were analyzed by gas chromatography (GC).

2.5 Analysis

The samples were analyzed by a gas chromatograph (Fuli, 9790) equipped with a DB-1 capillary column (30 m × 0.539 mm × 1.50 μm) and a hydrogen flame ionization detector (FID). The temperatures of injector and FID were all set at 250 °C.

3 Results and Discussions

3.1 Characterization

FT-IR spectra of catalysts were shown in Fig. 1. As can be seen in Fig. 1c, some peaks at wave number of 1079 cm^{-1} (P–O stretching vibration), 978 cm^{-1} (W=O stretching vibration), 893 cm^{-1} (W–O_b–W stretching vibration) and 805 cm^{-1} (W–O_c–W stretching vibration) were observed. The FT-IR spectra of [Bis–Bs–BDMAEE]$^{2+}HPW_{12}O_{40}^{2-}$ and $^1/_2$Cu[Bis–Bs–BDMAEE]$HPW_{12}O_{40}$ are similar, and also show that they all have peaks at wave number of 1079, 978, 893 and 805 cm^{-1}, showing they all retain the Keggin structure of $H_3PW_{12}O_{40}$. As shown in Fig. 1a, b, the bands at 3450 and 3014 cm^{-1} are attributed to the stretching vibration of O–H and C–H, respectively. The bands at 2927 and 2870 cm^{-1} are attributed to the stretching vibration of –CH_2–. The absorption peaks of 1479 cm^{-1} are attributed to bending vibration of –CH_2–. In addition, the peak at 1163 and 1043 cm^{-1} are assigned to the asymmetrical and symmetric stretching vibration of the –S=O

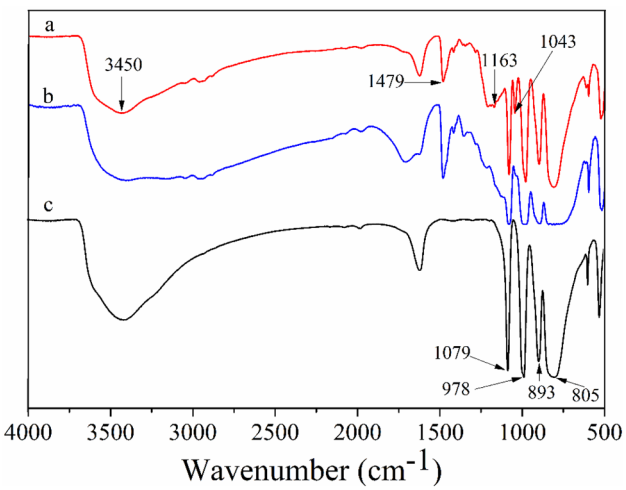

Fig. 1 FT-IR spectra for (a) $^1/_2$Cu[Bis–Bs–BDMAEE]$HPW_{12}O_{40}$, (b) [Bis–Bs–BDMAEE]$HPW_{12}O_{40}$, and (c) $H_3PW_{12}O_{40}$

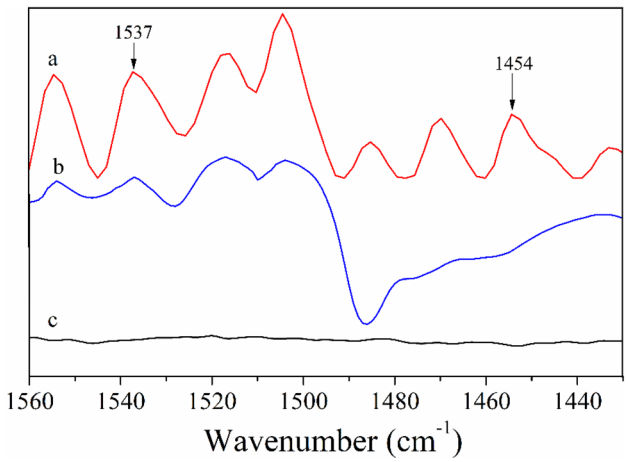

Fig. 2 Py-IR spectra of (a) $^{1}/_{2}$Cu[Bis–Bs–BDMAEE]HPW$_{12}$O$_{40}$, (b) [Bis–Bs–BDMAEE]PW$_{12}$O$_{40}$, and (c) CuO

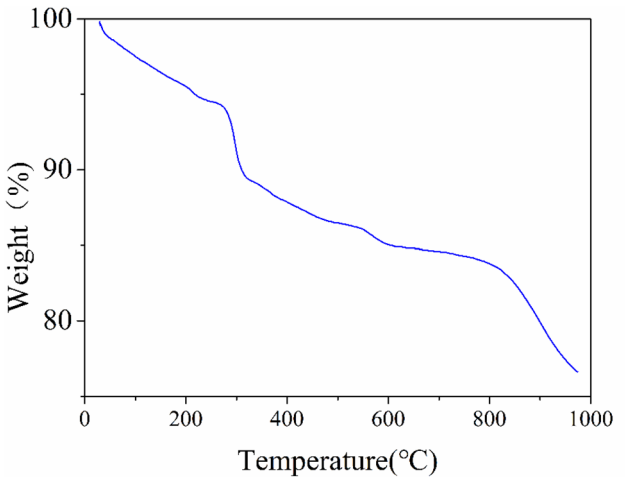

Fig. 3 TG curve of $^{1}/_{2}$Cu[Bis–Bs–BDMAEE]HPW$_{12}$O$_{40}$

to –SO$_3$H, respectively. The FT-IR spectra shows that both ILs of Fig. 1a, b not only preserve the Keggin structure of H$_3$PW$_{12}$O$_{40}$, while also retaining the organic cation structure.

Moreover, the Py-IR spectra illustrated in Fig. 2, which indicates that $^{1}/_{2}$Cu[Bis–Bs–BDMAEE]HPW$_{12}$O$_{40}$ exists both Brønsted acid sites (1537 cm^{-1}) and Lewis acid sites (1454 cm^{-1}), indicating that the presence of Brønsted–Lewis acidity derived from sulfonic acid groups and Cu^{2+}. [Bis–Bs–BDMAEE]PW$_{12}$O$_{40}$ only exists Brønsted acid sites, and Cuo has no any peaks.

The TG curve of [Bis–Bs–BDMAEE]HPW$_{12}$O$_{40}$ and $^{1}/_{2}$Cu[Bis–Bs–BDMAEE]HPW$_{12}$O$_{40}$ is shown in Fig. 3. The weight loss of catalyst is caused by evaporation of water in the sample before 250 °C. There are three obvious weightlessness after 250 °C, which shows that [Bis–Bs–BDMAEE] is gradually decomposed.

The SEM images of $^{1}/_{2}$Cu[Bis–Bs–BDMAEE]HPW$_{12}$O$_{40}$ were shown in Fig. 4, showing that catalyst have no definite morphology. In addition, X-ray energy spectrum (EDX) analysis was performed for $^{1}/_{2}$Cu[Bis–Bs–BDMAEE]HPW$_{12}$O$_{40}$ catalyst. As shown in Fig. 4b, which confirmed that the presence of Cu along with other elements (C, O, N, S, and W). The elemental analysis of the $^{1}/_{2}$Cu[Bis–Bs–BDMAEE]HPW$_{12}$O$_{40}$ is also carried out using an elemental analyzer. The measured results are as follows: C (6.53%), H (1.80%), O (21.68%), N (0.94%), S (2.08%), which is in agreement with the theoretical value of C (5.80%), H (1.19%), O (22.70%), N (0.85%), and S (1.94%).

3.2 Catalyst Performance

The esterification reaction of cyclohexene with acetic acid was investigated to test their catalytic activities under the same reaction conditions using different BLA-HPA- ILs and other acidic catalysts. The results were shown in Table 1.

First of all, the catalyst performance of the dual-sulfonic acid functionalized heteropolyacid based ionic liquids hybrid (HPA-ILs) with different heteropolyacid hybrid

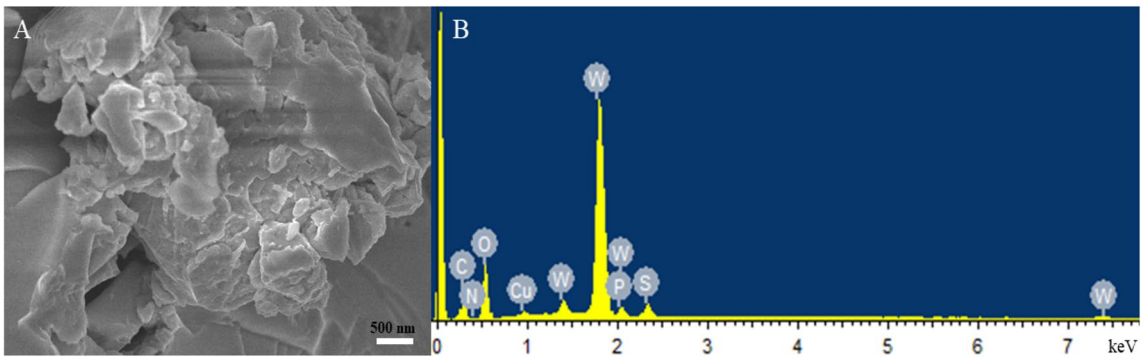

Fig. 4 The SEM (**A**) and EDX (**B**) of $^{1}/_{2}$Cu[Bis–Bs–BDMAEE]HPW$_{12}$O$_{40}$

Table 1 The esterification of cyclohexene with acetic acid on different catalysts

Entry	Catalysts	Conv.[a] (%)	Sel.[b] (%)	Yield.[c] (%)
1	[Bis–Bs–BDMAEE]$HPW_{12}O_{40}$	49.62	93.65	46.47
2	[Bis–Bs–BDMAEE]$HPMo_{12}O_{40}$	3.08	85.69	2.64
3	[Bis–Bs–BDMAEE]$H_2SiW_{12}O_{40}$	8.71	83.97	7.31
4	$^1/_4$Cu[Bis–Bs–BDMAEE]$HPW_{12}O_{40}$	53.28	93.75	49.95
5	$^1/_2$Cu[Bis–Bs–BDMAEE]$HPW_{12}O_{40}$	65.92	98.61	65.00
6	$^3/_4$Cu[Bis–Bs–BDMAEE]$HPW_{12}O_{40}$	44.94	97.41	43.78
7	Cu[Bis–Bs–BDMAEE]$HPW_{12}O_{40}$	40.16	97.10	39.00
8	$^{5/}{}_4$Cu[Bis–Bs–BDMAEE]$HPW_{12}O_{40}$	22.72	95.32	21.66
9	$^3/_2$Cu[Bis–Bs–BDMAEE]$HPW_{12}O_{40}$	2.30	66.93	15.39
10	$^1/_3$Fe[Bis–Bs–BDMAEE]$HPW_{12}O_{40}$	54.15	97.79	52.95
11	$^1/_3$Co[Bis–Bs–BDMAEE]$HPW_{12}O_{40}$	52.19	97.62	50.95
12	$^1/_2$Ni[Bis–Bs–BDMAEE]$HPW_{12}O_{40}$	51.10	95.09	48.59
13	$^1/_2$Zn[Bis–Bs–BDMAEE]$HPW_{12}O_{40}$	54.87	98.70	54.16
14	$^1/_3$Al[Bis–Bs–BDMAEE]$HPW_{12}O_{40}$	56.08	97.47	54.66
15	$H_3PW_{12}O_{40}$	51.32	94.02	48.25
16	$H_3PMo_{12}O_{40}$	41.91	92.85	38.91
17	$H_4SiW_{12}O_{40}$	52.81	94.98	50.16
18	H_2SO_4	46.49	98.12	45.62

[a]Conversion of cyclohexene

[b]Selectivity of cyclohexyl acetate

[c]Yield of cyclohexyl acetate. Reaction conditions: temperature = 363.15 K, catalyst dosage = 7 wt.% (based on the mass of all reactants), acetic acid/cyclohexene molar ratio = 3.0, and reaction time = 7.0 h

anions was investigated for determining the best heteropolyacid hybrid anion. As can be seen in Table 1 (entries 1–3), [Bis–Bs–BDMAEE]$HPW_{12}O_{40}$ shows the best catalytic performance compared with the other two catalysts, and the conversion of cyclohexene and the selectivity of cyclohexyl acetate reached 49.62% and 93.65%, respectively. The BLA-HPA-ILs with Brønsted acid and Lewis acid by adding the different metals (M = Cu, Fe, Co, Ni, Zn, Al) into the [Bis–Bs–BDMAEE]$HPW_{12}O_{40}$ catalyst. As shown in Table 1 (entries 4–14), $^1/_2$Cu[Bis–Bs–BDMAEE]$HPW_{12}O_{40}$ catalyst shows the most excellent catalytic performance compared to other transition metal doped catalysts. The conversion of cyclohexene, cyclohexyl acetate selectivity and yield reached 65.92%, 98.61% and 65.00%, respectively (entry 5). This may be due to that doped metal Cu with Lewis acidity can enhance the formation of carbon cations. The reaction mechanism of esterification of cyclohexene was shown in Scheme 2. The reaction of cyclohexene with acid first generates carbocation intermediate, and then the carbocation intermediate further reacts with acetic acid to generate cyclohexyl acetate. It can be seen that the key rate step of esterification is the generation of the carbocation intermediate in the first step. For Brønsted acid, its proton H^+ reactions with cyclohexene easily to generate more carbenium ion, which makes the reaction rate faster. However, carbenium ion may also react with cyclohexene, generating cyclohexene dimer by-products (Scheme 2a). This results indicate that Brønsted acid catalysts can generate the more carbocation intermediate to accelerate conversion of cyclohexene, and reduce the selectivity of cyclohexyl acetate simultaneously. For Lewis acid, the reaction mechanism is that the vacant orbital of Lewis acid is coordinated with π–π electron cloud of cyclohexene, inducing cyclohexene to form carbocation intermediate, resulting in slower rate of carbocation intermediate generation (Scheme 2b). The overall rate of esterification reaction becomes slower, and the side reactions are also decreased at the same time. So, the BLA-HPA-ILs with Brønsted–Lewis acid sites may increase the conversion of the cyclohexene and the selectivity of target product cyclohexyl acetate by synergistic effect between Brønsted acid and Lewis acid.

The contents of Brønsted acid and Lewis acid have important influence on catalytic activity of the catalyst. Therefore, BLA-HPA-ILs with different content of Brønsted acid and Lewis acid were prepared by adding different amount of Cu, and the catalytic performance was shown in entries 4–9. Interestingly, the conversion of cyclohexene and the selectivity of cyclohexyl acetate increases with the addition of the metal Cu. When $^1/_2$Cu[Bis–Bs–BDMAEE]$HPW_{12}O_{40}$ is used as a catalyst, the catalytic activity is optimal. However, the BLA-HPA-ILs catalytic activity began to decline with the amount of Cu further increase (entries 6–9), which increase the content of Lewis acid. This is may be due to that the

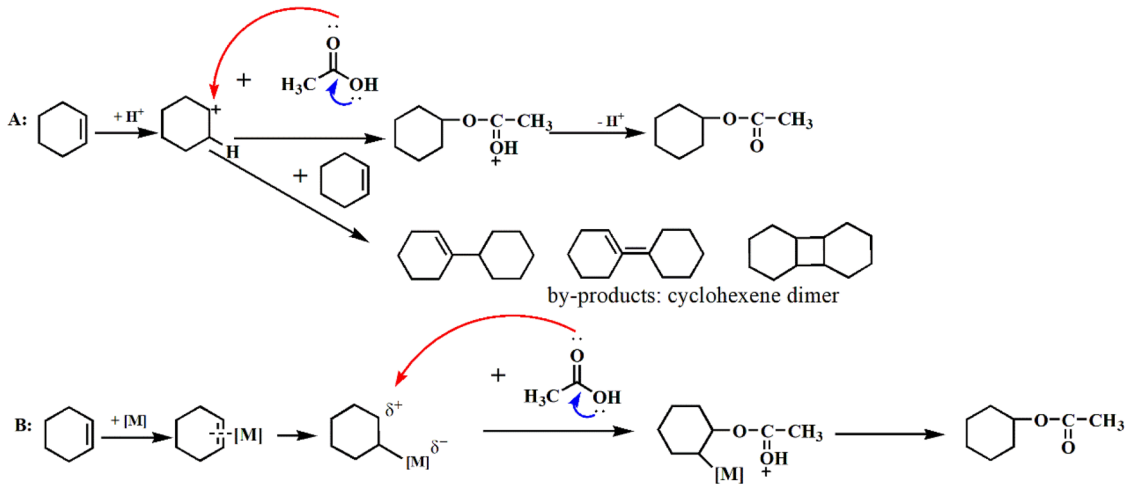

Scheme 2 Mechanism of esterification of cyclohexene catalyzed by (**A**) Brønsted acid and (**B**) Lewis acid

large amount of Cu added can hinder the nucleophilic attack of acetic acid, leading to reduce the conversion of cyclohexene.

The conventional acidic catalyst sulfuric acid, $H_3PW_{12}O_{40}$, $H_3PMo_{12}O_{40}$ and $H_4SiW_{12}O_{40}$ showed relatively low catalytic performance (entries 15–18). In addition, these conventional acidic catalysts have some disadvantages such as difficult separation from the reaction mixtures, environmental pollution. However, as heterogeneous catalysts, BLA-HPA-ILs can be easily separated from the reaction mixtures via simple filtration. In a word, $^1/_2$Cu[Bis–Bs–BDMAEE]$HPW_{12}O_{40}$ was found to have promising application in esterification of cyclohexene with acetic acid.

3.3 Effect of Reaction Temperature

As shown in Fig. 5, the conversion of cyclohexene at different reaction temperatures in the range of 333.15 to 363.15 K was studied using $^1/_2$Cu[Bis–Bs–BDMAEE]$HPW_{12}O_{40}$ under the same reaction conditions. The conversion of cyclohexene at 7 h increased obviously from 28.89 to 65.92% when the reaction temperature was increased from 333.15 to 363.15 K, indicating that an increase in reaction temperature is beneficial in enhancing the conversion of cyclohexene. This means that the increase of temperature is helpful to the improvement of the reaction rate, which is due to the temperature increase may lead to more successful collisions between reactants. On this account, there is sufficient energy to break the bonds to form products, which leads to a higher conversion rate of cyclohexene.

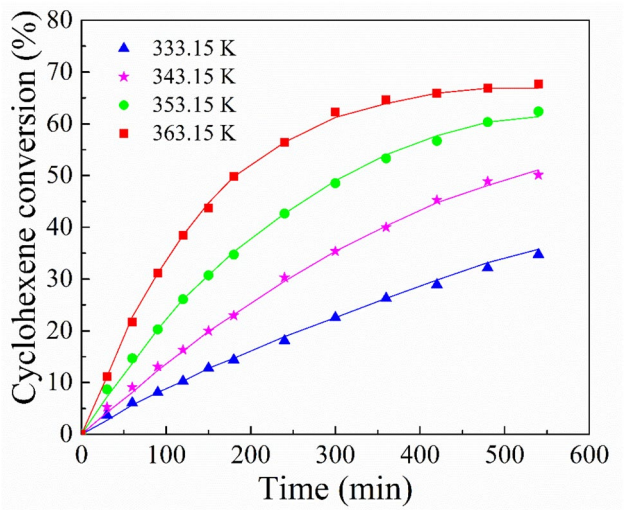

Fig. 5 Effect of reaction temperature on the conversion of cyclohexene using $^1/_2$Cu[Bis–Bs–BDMAEE]$HPW_{12}O_{40}$ as catalyst. Reaction conditions: catalyst dosage = 7 wt.%, acetic acid/cyclohexene molar ratio = 3.0

3.4 Effect of Catalyst Dosage

The effect of different catalyst dosage on the conversion of cyclohexene in the range of 3 to 9 wt.% was investigated using $^1/_2$Cu[Bis–Bs–BDMAEE]$HPW_{12}O_{40}$ as catalyst under the same reaction conditions. As shown in Fig. 6, it can be observed that the conversion of cyclohexene increased with increasing catalyst dosage from 3 to 7 wt.%. This is due to the increased catalyst dosage can improve the active ingredient concentration, and lead to speed up the reaction rate. The conversion of cyclohexene at 7 h increased from 38.34 to 65.92% when catalyst dosage was increased from 3 to

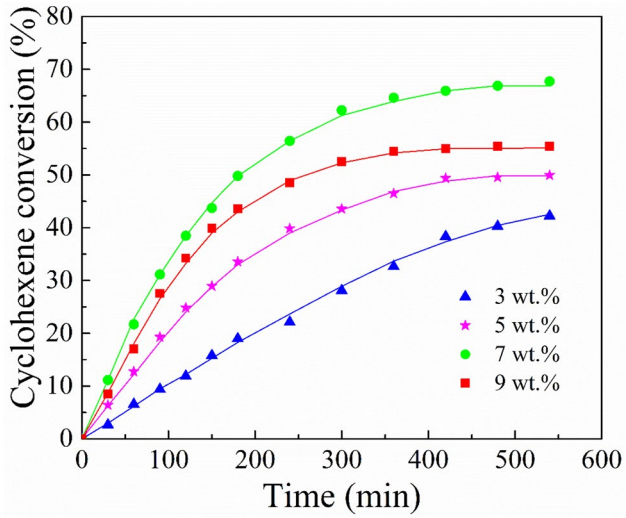

Fig. 6 Effect of catalyst dosage on the conversion of cyclohexene using $^{1}/_{2}$Cu[Bis–Bs–BDMAEE]HPW$_{12}$O$_{40}$ as catalyst. Reaction conditions: temperature = 363.15 K, acetic acid/cyclohexene molar ratio = 3.0

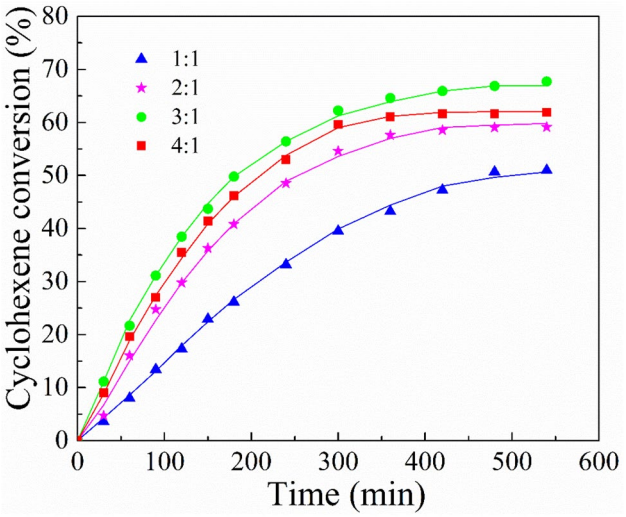

Fig. 7 Effect of initial reactant molar ratio on the conversion of cyclohexene using $^{1}/_{2}$Cu[Bis–Bs–BDMAEE]HPW$_{12}$O$_{40}$ as catalyst. Reaction conditions: temperature = 363.15 K and catalyst dosage = 7 wt.%

7 wt.%. However, the conversion of cyclohexene begins to decrease with further increase of the catalyst dosage from 7 to 9 wt.%. This might be because the mass transfer resistance increases with further increase of the catalyst dosage under the same stirring conditions. There a low reaction rate was obtained thanks to a low mass transfer coefficient with further increase of the catalyst dosage under the same stirring conditions, resulting in a lower reaction conversion rate. Moreover, the amount of catalyst was further increased, the catalyst easily forms a pile in the reaction system, which can reduce contact between the active sites of catalysts and reactants, leading to the lower conversion of cyclohexene. As a consequence, excessive amounts of catalyst are disadvantageous to the esterification of cyclohexene, and the optimal catalyst dosage is 7 wt.%.

3.5 Effect of Initial Reactant Molar Ratio

The effect of initial reactant molar ratio on the conversion of cyclohexene was investigated using $^{1}/_{2}$Cu[Bis–Bs–BDMAEE]HPW$_{12}$O$_{40}$ as catalysts under the same reaction conditions. As can be seen in Fig. 7, the conversion of cyclohexene increased obviously with the molar ratio changed from 1:1 to 3:1. This is because an increase in the concentration of acetic acid brings the reaction toward positive reaction side for this reversible reaction. However, when the molar ratio was further increased from 3:1 to 4:1, the conversion of cyclohexene decreased from 65.92 to 61.63%. This may be ascribed to the fact that the concentration of cyclohexene can be diluted when the amount of acetic acid was further increased. Therefore, an excess of acetic acid is not conducive to the esterification of cyclohexene, and the optimal molar ratio is 3:1.

3.6 Chemical Equilibrium

The esterification reaction equation of cyclohexene with acetic acid can be written as follows:

$$A + B \underset{k_-}{\overset{k_+}{\rightleftharpoons}} D \tag{1}$$

Here, A is cyclohexene, B is acetic acid and D is cyclohexyl acetate. Kinetic experiments were carried out to obtain the chemical equilibrium constants under the same conditions at different temperatures. Samples were taken out of the reactor after specific time intervals for analyzed until chemical equilibrium was reached. The chemical equilibrium constants were calculated via Eq. (2):

$$K_e = \frac{C_D}{C_A C_B} \tag{2}$$

Here K_e represents the equilibrium constant; C_i is the equilibrium concentration of component i (mol L^{-1}).

The dependency of the equilibrium constant K_e on the temperature can be found from a plot of ln K_e versus the reciprocal temperature ($1/T$), as given in Fig. 8. It was found that the equilibrium constant decreased with increasing temperature, indicates the esterification reaction of cyclohexene with acetic acid is an exothermic reaction. The equilibrium constant as shown in Eq. (3) can be expressed as follows:

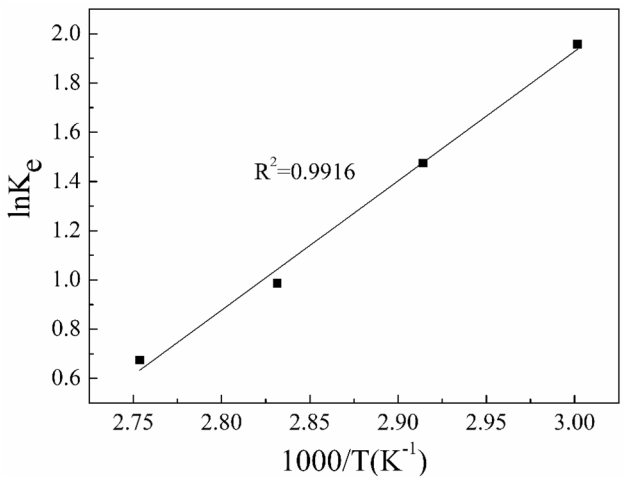

Fig. 8 Effects of reaction temperature on the chemical equilibrium constant

$$\ln K_e = \frac{5256.2}{T} - 13.84 \tag{3}$$

The reaction enthalpy ($\Delta_r H^0$) and entropy ($\Delta_r S^0$) were estimated via the van't Hoff equation [52, 53]:

$$\ln K_e = \frac{-\Delta_r H^0}{RT} + \frac{\Delta_r S^0}{R} \tag{4}$$

The reaction enthalpy ($\Delta_r H^0$) and entropy ($\Delta_r S^0$) were found to be − 43.70 kJ mol^{-1} and − 115.07 J mol^{-1} K^{-1} in this work, respectively. The negative reaction enthalpy again indicates that this esterification reaction of cyclohexene with acetic acid is the exothermic reaction.

3.7 Reaction Kinetic Model

A pseudohomogeneous (PH) model can be used to express many esterification reactions systems where one of the reactants or solvents is highly polar [54–56]. In this work, the kinetic equation for the reversible esterification reaction of cyclohexene with acetic acid was established according to the PH model, which can be written as Eq. (5):

$$r = -\frac{dC_A}{dt} = m_{cat}\left(k_+ C_A C_B - k_- C_D\right) = m_{cat} k_+ \left(C_A C_B - \frac{C_D}{K_e}\right) \tag{5}$$

Here $K_e = k_+/k_-$ is the equilibrium constant; m_{cat} is the catalyst dosage per unit volume; C_i is the molar concentration of component i; k_+ and k_- are the rate constants of the forward and reverse reactions, respectively.

The kinetic equation was integrated by a fourth-order Runge–Kutta method. The kinetic parameters were estimated by minimizing the sum of residual squares (*SRS*) between the values for the conversion of cyclohexene calculated according to the PH model and obtained by experiments, as shown in Eq. (6):

$$SRS = \sum_{Samples} \left(x_{\exp} - x_{calc}\right)^2 \tag{6}$$

where *SRS* is the minimum sum of residual squares and x is the conversion of cyclohexene. The subscripts *exp* and *cal* represent experimental and calculated values, respectively. According to the calculated results, it was revealed that the conversions of cyclohexene calculated by the reaction kinetic model were very consistent with those obtained from the experiments. The comparison data between the calculated results and the experimental results are shown in Figs. 9, 10, and 11.

Therefore, the PH model provides a good description of the kinetic behavior for the esterification of cyclohexene with acetic acid using $^1/_2$Cu[Bis–Bs–BDMAEE]HPW$_{12}$O$_{40}$ as catalysts.

The effect of the temperature on the reaction rate constants in this work can be expressed by the Arrhenius equation as follows:

$$\ln k = \ln k_0 - \frac{E_a}{RT} \tag{7}$$

The activation energy (E_a) and pre-exponential factor (k_0) were obtained by the relationship between ln$k$ and $1/T$ from Eq. (7). As shown in Fig. 12, the intercept on the ordinate (ln k_0) and the slope of straight lines ($-E_a$

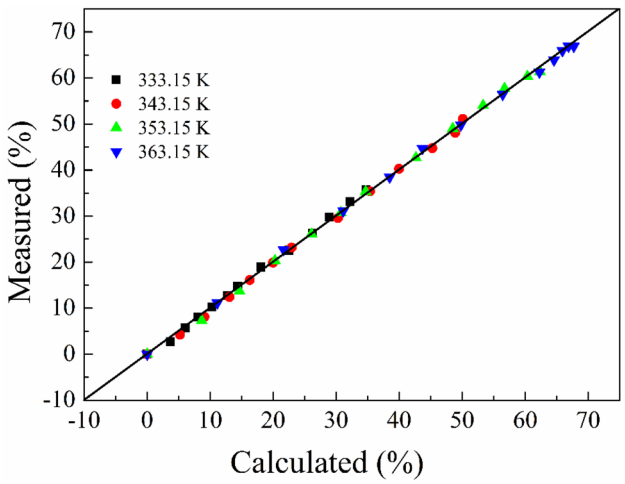

Fig. 9 Comparison between measured and calculated at different temperatures using $^1/_2$Cu[Bis–Bs–BDMAEE]HPW$_{12}$O$_{40}$ as catalyst. Reaction conditions: catalyst dosage = 7 wt.%, acetic acid/cyclohexene molar ratio = 3.0

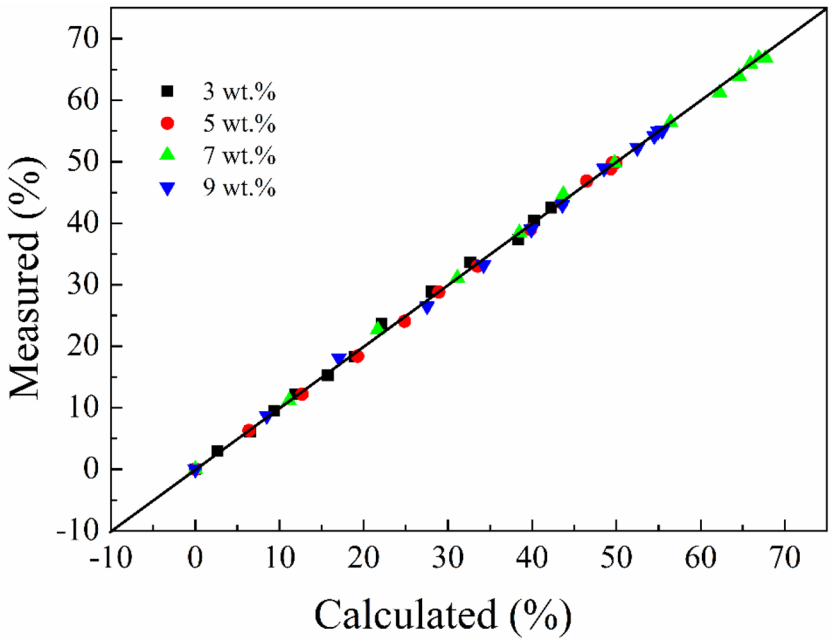

Fig. 10 Comparison between measured and calculated at different catalyst dosage using $^1/_2$Cu[Bis–Bs–BDMAEE]$HPW_{12}O_{40}$ as catalyst. Reaction conditions: temperature = 363.15 K, acetic acid/cyclohexene molar ratio = 3.0

/*R*) were obtained. The activation energy (E_a) and pre-exponential factor (k_0) were listed in Table 2. The kinetic data obtained has promising prospects for designing the esterification process of cyclohexene with acetic acid and also providing an optimal setup of various operating parameters.

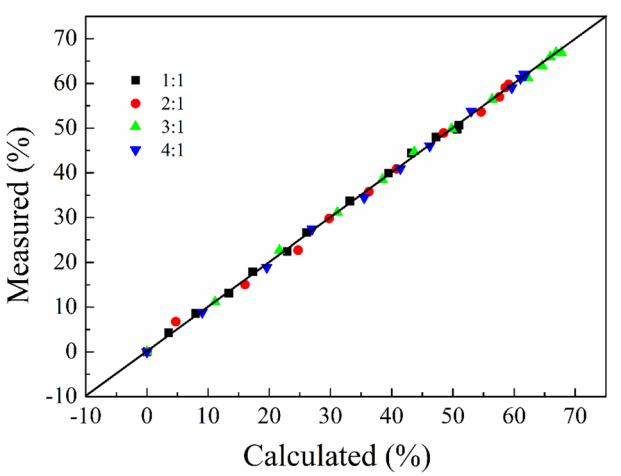

Fig. 11 Comparison between measured and calculated at different initial reactant molar ratio using $^1/_2$Cu[Bis–Bs–BDMAEE]$HPW_{12}O_{40}$ as catalyst. Reaction conditions: temperature = 363.15 K and catalyst dosage = 7 wt.%

3.8 Reusability of Catalyst

The stability and reusability of catalysts are important factors for the application in industry. The reusability of BLA-HPA-ILs $^1/_2$Cu[Bis–Bs–BDMAEE]$HPW_{12}O_{40}$ in the esterification reaction of cyclohexene and acetic acid were studied in detail. These reactions are liquid–solid biphasic heterogeneous reactions by using $^1/_2$Cu[Bis–Bs–BDMAEE]$HPW_{12}O_{40}$ as catalysts, so the solid catalyst could be easily recycled by simple filtration. After washing for three times using acetone and drying at 80 °C for 12 h under a vacuum, the catalyst can be used to the next run directly. As shown in Fig. 13, after reusing the catalysts of $^1/_2$Cu[Bis–Bs–BDMAEE]$HPW_{12}O_{40}$ six times, the selectivity of cyclohexyl acetate is almost unchanged, and the conversion of cyclohexene has a slight decrease, which is may be due to the loss of the catalysts in the treatment process. As shown in Fig. 14, the FT-IR spectra of the fresh BLA-HPA-ILs and the repeatedly used six times catalyst. It shows that the peaks of both catalysts are similar, which indicates that the structure of the BLA-HPA-ILs is extremely stable after reuse for six cycles. Therefore, the BLA-HPA-ILs acidic active sites are not easily lost and its reusability is excellent.

4 Conclusions

A series of BLA-HPA-ILs were synthesized by combining the Brønsted acidic ionic liquid [Bis–Bs–BDMAEE]$HPW_{12}O_{40}$ with metallic oxide in different composition ratios and applied in the esterification of cyclohexene with acetic acid to produce cyclohexyl acetate. Compared with BLA-HPA-ILs catalysts with doping other metallic oxide, HPA-ILs, H_2SO_4, $H_3PW_{12}O_{40}$, $H_3PMo_{12}O_{40}$ and

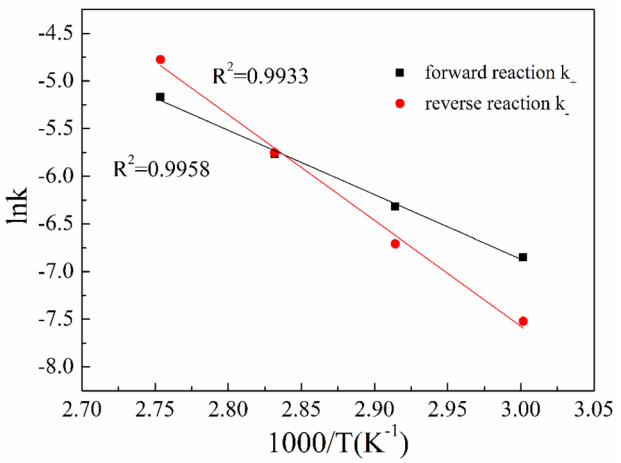

Fig. 12 Arrhenius plots for the esterification of cyclohexene with acetic acid using $^{1}/_{2}$Cu[Bis–Bs–BDMAEE]HPW$_{12}$O$_{40}$ as catalysts

Table 2 Parameters of the PH model

Reaction	k_0 (L^2 mol^{-2} min^{-1})	E_a (kJ mol^{-1})
Forward reaction	6.68×10^5	56.21
Reverse reaction	1.52×10^{11}	92.34

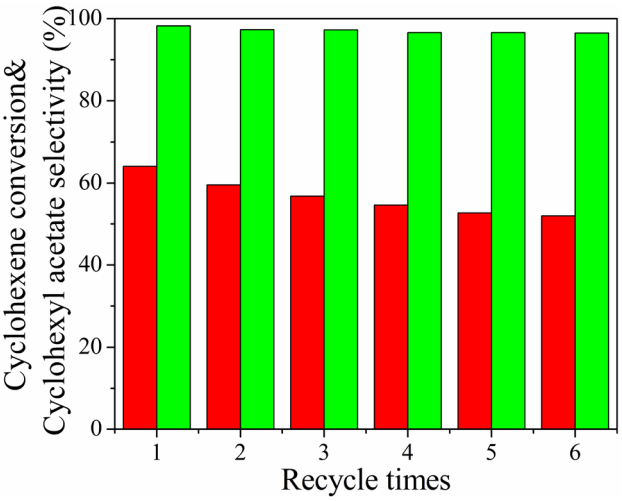

Fig. 13 Conversion rate (red column) and selectivity (green column) of $^{1}/_{2}$Cu[Bis–Bs–BDMAEE]HPW$_{12}$O$_{40}$. Reaction conditions: temperature = 363.15 K, catalyst dosage = 7 wt.%, acetic acid/cyclohexene molar ratio = 3.0, and reaction time = 7.0 h

$H_4SiW_{12}O_{40}$, $^{1}/_{2}$Cu[Bis–Bs–BDMAEE]HPW$_{12}$O$_{40}$ were found to have the most excellent catalytic activity and the conversion of cyclohexene and cyclohexyl acetate selectivity reached 65.92% and 98.61%, respectively. In addition, the pseudohomogeneous (PH) reaction kinetic model was applied to correlate the experimental data and the kinetic parameters were estimated. The calculated results are in good agreement with the experimental results, indicating the PH model gives a good representation of the kinetic behavior for the esterification of cyclohexene. In a word, $^{1}/_{2}$Cu[Bis–Bs–BDMAEE]HPW$_{12}$O$_{40}$ catalyst possess the excellent stability and reusability, showing promising potential for application in industry.

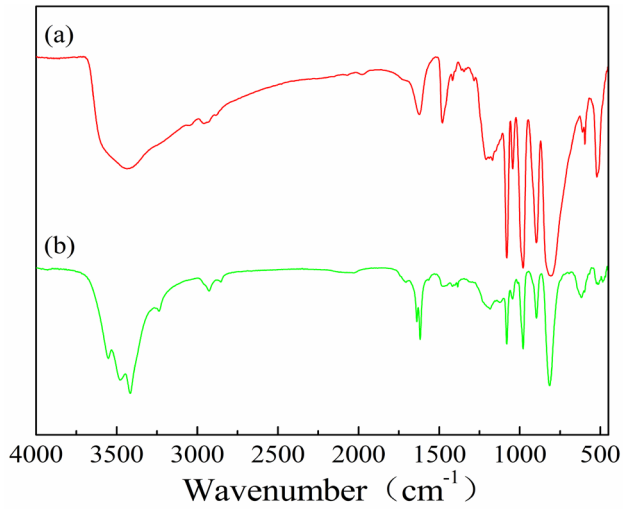

Fig. 14 FT-IR spectra of $^{1}/_{2}$Cu[Bis–Bs–BDMAEE]HPW$_{12}$O$_{40}$: (a) the fresh catalyst and (b) reused six times catalyst

Acknowledgements This work was supported by the National Natural Science Foundations of China (No. 21676072), Henan Science and Technology Research Project (212102210653, 202102310285), China Postdoctoral Science Foundation (2020M672209), and Scientific Research Projects for Higher Education of Henan Province (20A530002), the Program for Innovation Teams in Science and Technology in Universities of Henan Province (20IRTSTHN004).

Declarations

Conflict of interest The authors declare that they have no known competing financial interests or personal relationships that could have appeared to influence the work reported in this paper.

References

1. Xiang YZ, Li XN (2007) J Chem Ind Eng 58:3041–3045
2. Ishida H (1997) Catal Surv 1:241–246
3. Fang CX, Yu Y, Wang YT, Qu YX (2012) Mod Chem Ind 32:16–19
4. Wu JM, Dai XM, Chen JL, Guo WD (2003) Chem Ind Eng Prog 22:1222–1224
5. Fang DR, Lu JY, Zhang HM, Li J, Wang YY (2013) Chem Res Chin Univ 29:743–746
6. Jin JJ, Li F, Yang LH, Zhang DS, Xue W, Wang YJ (2004) Acta Petrol Sin (Pet Process Section) 30:169–174

7. Guo ZW, Jin HB, Tong ZM (2006) Chem Ind Eng Prog 25:852–859
8. Wang BY, Ge XX, Wu FL, Wu YX, Zheng HD, Qiu T (2010) Chem Ind Eng Prog 29:861–865
9. Zhang H, Mahajani SM, Sharma MM, Sridhar T (2002) Chem Eng Sci 57:315–322
10. Katariya A, Freund H, Sundmacher K (2009) Ind Eng Chem Res 48(21):9534–9545
11. Xue W, Zhao HP, Yao J, Li F, Wang YJ (2016) Chin J Catal 37(5):769–777
12. Cao ZJ, Zhao X, He FQ, Zhou Y, Huang K, Zheng AM, Tao DJ (2018) Ind Eng Chem Res 57(19):6654–6663
13. Steyer F, Freund H, Sundmacher K (2008) Ind Eng Chem Res 47:9581–9587
14. Sang HL, Won YC, Kyung JK, Dae JC, Jae WL (2018) Chem Eng Process 123:249–257
15. Rakesh K, Amit K, Hannsjorg F, Kai S (2011) Org Process Res Dev 15:527–539
16. Yao B, Wang Z, Xiao T, Cao F, Edwards PP (2015) Appl Petrochem Res 5:135–142
17. Zheng GC, Li XZ (2019) Synth Commun 49(7):1–9
18. Jiang HR, Lu B, Ma LJ, Yuan X (2020) Catal Lett 150:1786–1797
19. Ma L, Xu L, Jiang H, Yuan X (2019) RSC Adv 9:5692–5700
20. Lu B, Wu ZW, Ma LJ, Yuan X (2018) J Taiwan Inst Chem Eng 88:1–7
21. Zhang QH, Zhang SG, Deng YQ (2011) Green Chem 13:2619–2637
22. Chen FF, Huang K, Zhou Y, Tian ZQ, Zhu X, Tao DJ, Jiang DE, Dai S (2016) Angew Chem Int Ed 55:7166–7170
23. Song ZB, Huang W, Zhou Y, Tian ZQ, Li ZM, Tao DJ (2020) Green Chem 22:103–109
24. Hui W, Zhou Y, Dong Y, Cao ZJ, He FQ, Cai MZ, Tao DJ (2019) Green Energy Environ 4:49–55
25. Yang F, Xue W, Zhang DS, Li F, Wang YJ (2016) React Kinet Mech Catal 117:329–339
26. Tao DJ, Dong Y, Cao ZJ, Chen FF, Chen XS, Huang K (2016) J Ind Eng Chem 41:122–129
27. Yang Z, Cui XB, Jie HM, Yu XF, Zhang Y, Feng TY, Liu H, Song K (2015) Ind Eng Chem Res 54:1204–1251
28. Ou YF, Wang ZZ, Zhou Y, Chen Z, Lu ZH, Yang Z, Tao DJ (2015) Appl Catal A 492:177–183
29. An XC, Li ZM, Zhou Y, Zhu WS, Tao DJ (2020) Chem Eng J 394:124859
30. Cai XJ, Cui SH, Qu LP, Yuan DD, Lu B, Cai QH (2007) Catal Commun 9:6
31. Hafizi A, Ahmadpour A, Koolivand-Salooki M, Heravi MM, Bamoharram FF (2013) J Ind Eng Chem 19:1981–1989
32. Sawant DP, Vinu A, Justus J, Srinivasu P, Halligudi SB (2007) J Mol Catal A 276:150–157
33. Zhou Y, Chen GJ, Long ZY, Wang J (2014) RSC Adv 4:42092–42113
34. Liu YY, Murata K, Inaba M (2006) J Mol Catal A 256:247–255
35. Leng Y, Wang J, Zhu DR, Shen L, Zhao P, Zhang M (2011) Chem Eng J 173:620–626
36. Leng Y, Wang J, Zhu DR, Ren XQ, Ge HQ, Shen L (2009) Angew Chem Int Ed 48:168–171
37. Li KX, Chen L, Wang HL, Lin WB, Yan ZC (2011) Appl Catal A 392:233–237
38. Zhao PP, Zhang MJ, Wu YJ, Wang J (2012) Ind Eng Chem Res 51:6641–6647
39. Leng Y, Zhao PP, Zhang MJ, Wang J (2012) J Mol Catal A 358:67–72
40. Zhao PP, Leng Y, Wang J (2012) Chem Eng J 204:72–78
41. Huang WL, Zhu WH, Li HM, Shi H, Zhu GP, Liu H, Chen GY (2010) Ind Eng Chem Res 49:8998–9003
42. Liu Y, Wang TY, Zhai CP, Chen WP, Qiao CZ (2014) Ind Eng Chem Res 53:14633–14640
43. Liu Y, Liu WH, Shao XN, Wang JH, Li XY (2018) Catal Lett 148:144–153
44. Liu Y, Liu WH, Wang L, Su MJ, Liu FJ (2018) Ind Eng Chem Res 57:5207–5214
45. Matuszek K, Chrobok A, Coleman F, Seddonb KR, Kwaśny MS (2014) Green Chem 16:3463–3471
46. Wang HX, Wu CM, Bu XW, Tang WL, Li L, Qiu T (2014) Chem Eng J 246:366–372
47. Yang YB, He WS, Jia CS, Ma Y, Zhang XM, Feng B (2012) J Mol Catal A 357:39–43
48. Han XX, Yan W, Hung CT, Liu LL, Wu PH, Ren DH, Huang SJ, Liu SB (2016) Korean J Chem Eng 33:2063–2072
49. Liu SW, Chen CG, Yu FL, Li L, Liu ZG, Yu ST, Xie CX, Liu FS (2015) Fuel 159:803–809
50. Yuan B, Xie CX, Yu FL, Yang XY, Yu ST, Zhang JL, Chen XB (2016) Springer Plus 5:460–464
51. Liu Y, Wu YF, Su MJ, Liu WH, Li XY, Liu FJ (2020) J Ind Eng Chem 92:200–209
52. Tao DJ, Li ZM, Cheng Z, Hu N, Chen XS (2012) Ind Eng Chem Res 51:16263–16269
53. JagadeeshBabu PE, Sandesh K, Saidutta MB (2011) Ind Eng Chem Res 50:7155–7160
54. Jignesh G, Surendra M, Sanjay M (2003) Ind Eng Chem Res 42:2146–2155
55. Bastian S, Michael D, Julrgen G (2008) Ind Eng Chem Res 47:698–703
56. Tsai YT, Lee MJ (2011) Ind Eng Chem Res 50:1171–1176

Authors and Affiliations

Binxiong Guang[1] · Yuefeng Wu[1] · Weihua Liu[1] · Jianhong Wang[1] · Yahui Xiao[1] · Yong Liu[1]

[1] Henan Key Laboratory of Polyoxometalate Chemistry, College of Chemistry and Chemical Engineering, Henan University, Kaifeng 475004, People's Republic of China